Editors' Suggestion

Perturbative analysis of quasiperiodic patterning of transmon quantum computers: Enhancement of many-body localization

Evangelos Varvelis [1,2,*] and David P. DiVincenzo [1,2,3]

[1]*Institute for Quantum Information, RWTH Aachen University, 52056 Aachen, Germany*

[2]*Jülich-Aachen Research Alliance (JARA), Fundamentals of Future Information Technologies, 52425 Jülich, Germany*

[3]*Peter Grünberg Institute, Theoretical Nanoelectronics, Forschungszentrum Jülich, 52425 Jülich, Germany*

(Received 23 December 2022; revised 22 March 2024; accepted 22 March 2024; published 10 April 2024)

Recently, it has been shown that transmon qubit architectures experience a transition between many-body localized and quantum chaotic phases. While it is crucial for quantum computation that the system remains in the localized regime, the most common way to achieve this has been relying on disorder in Josephson junction parameters. Here, we propose a quasiperiodic patterning of parameters as a substitute for random disorder. We demonstrate, using the Walsh-Hadamard diagnostic, that quasiperiodicity is more effective than disorder for achieving localization. To study the localizing properties of our Hamiltonian for large, experimentally relevant system sizes, we use two complementary perturbation theory schemes, one with respect to the many-body interactions and one with respect to the hopping parameter of the free Hamiltonian.

DOI: 10.1103/PhysRevB.109.144201

I. INTRODUCTION

Despite immense advances in quantum computing using the superconducting qubit platform [1–3], two-qubit gate fidelity remains a thorn in the side of further progress with these devices. One prominent source of these errors is quantum crosstalk in the form of qubit ZZ couplings [4], with Z denoting the Pauli z operator. This crosstalk is the result of always-on coupling of qubits, even in idle mode. There are two primary strategies for dealing with these residual couplings: tunable coupling [5] and static coupling between opposite anharmonicity qubits [6,7]. Each of these comes with disadvantages: additional hardware overlay of couplers for the former and lower coherence time of capacitively shunted flux qubits for the latter. In real devices, the existence of natural random disorder is unavoidable and most prominently present in the critical current of Josephson junctions. Even though in modern devices tuning of Josephson junctions is possible, even postfabrication, with laser annealing techniques [8], some degree of residual disorder remains.

The many-body system formed by a network of N Josephson qubits, with random disorder and fixed coupling, is a prime candidate for quantum chaos. Recently, it has been established that there is in fact a phase transition between quantum chaotic and many-body localization (MBL) for transmon arrays [9] of this type. The phenomenology of this transition can be summarized by considering the diagonalized Hamiltonian of such a multiqubit system:

$$H = \sum_{a\in\mathbb{B}^N} E_a|a\rangle\langle a| = \sum_{b\in\mathbb{B}^N} w_b Z_1^{b_1}\dots Z_N^{b_N}, \tag{1}$$

where $\mathbb{B}^N$ is the set of all bit-strings of length N, w_b is a real coefficient corresponding to bit-string b, b_i is the ith digit of bit-string b, and Z_i is the Pauli z operator acting on the subspace of qubit i. The coefficients w_b with a bit-string b consisting of only two 1's in adjacent sites correspond, by definition, to the ZZ couplings. Longer-range ZZ couplings or higher-weight terms have generally been neglected (but see Ref. [10]), a treatment that is consistent in the MBL phase, where we have an exponential hierarchy of these terms with respect to correlation range [11,12]. This is in stark contrast with the chaotic regime, however, where all of these terms are of the same order of magnitude.

These systems can only be deep in the MBL phase due to the happenstance of disorder in the energies E_J of the Josephson qubits. In this paper, we explore the stabilization of the MBL phase with a quasiperiodic potential replacing the randomly chosen disorder potential and determine that there is in fact a robust localized regime. We demonstrate this for a small system by obtaining the inverse participation ratio and the Walsh-Hadamard coefficients w_b of Eq. (1) using exact diagonalization techniques. To obtain the latter, we apply the Walsh-Hadamard transform on the spectrum of the system:

$$w_b = \frac{1}{2^N}\sum_{a\in\mathbb{B}^N}(-1)^{b\cdot\bar{a}}E_a, \tag{2}$$

with $\bar{a}$ denoting a bit-string resulting from flipping each digit of bit-string a [13].

To extend our results to system sizes comparable with currently available devices, we will use a two-track analytic approach. On the one hand, we develop a bosonic variant of Møller-Plesset (MP) perturbation theory [14], treating the many-body interactions as the small parameter. On the other hand, we also use standard Rayleigh-Schrödinger (RS) perturbation theory in the hopping strength. For both schemes, we obtain the energy levels of the qubit sector of the system and consequently, from these, the Walsh-Hadamard coefficients from a direct application of the definition in Eq. (2). The use of both schemes is necessitated by the fact that, while the MP

*evangelos.varvelis@rwth-aachen.de

perturbation theory scheme allows us to obtain longer-range correlations, it is only valid deep in the localized regime. On the contrary, the RS perturbation theory scheme is more accurate for a broader region of the MBL regime, but obtaining longer-range correlations requires progressively higher orders of perturbation theory, rendering their calculation within this scheme impractical.

II. METALLIC AUBRY-ANDRÉ MODEL

Here, we focus on capacitively coupled transmon arrays. The minimal model Hamiltonian for such an array [15,16] is

$$H = 4E_{\mathrm{C}} \sum_{i=1}^{N} n_i^2 - \sum_{i=1}^{N} E_{\mathrm{J}_i} \cos(\phi_i) + \lambda \sum_{\langle i,j \rangle} n_i n_j, \qquad (3)$$

where n_i is the Cooper-pair number of site i, and ϕ_i is the conjugate variable, corresponding to the superconducting phase. Here, E_{C} is the capacitive energy of each transmon, taken to be equal for all sites of the array, E_{J_i} is the Josephson energy of site i, and λ is the constant coupling strength between sites. We also assumed only nearest-neighbor coupling.

After recasting the Hamiltonian of Eq. (3) in second quantization form and expanding the cosine term up to fourth order to include many-body interactions via the anharmonicity, we obtain the Bose-Hubbard approximation of our Hamiltonian:

$$H_{\mathrm{BH}} = \sum_{i=1}^{N} \omega_i a_i^\dagger a_i + J \sum_{\langle i,j \rangle} a_i^\dagger a_j - \frac{E_{\mathrm{C}}}{2} \sum_{i=1}^{N} a_i^\dagger a_i^\dagger a_i a_i. \qquad (4)$$

We have also used a rotating wave approximation. Note that the ladder operators are bosonic—we are not restricted to the single-excitation manifold of the Fock space. Strictly speaking, the new coupling strength J would be bond dependent and proportional to $\lambda\sqrt{\omega_i\omega_j}/E_{\mathrm{C}}$, with $\omega_i = \sqrt{8E_{\mathrm{J}_i}E_{\mathrm{C}}} - E_{\mathrm{C}}$. Here, we have omitted this bond dependence to simplify the calculations. We find that including this dependence does not substantially alter our results.

To design a frequency pattern ω_i for our transmon arrays, which should serve in place of a localizing disorder potential, the essential feature is to make it nonrepeating to avoid resonances. A secondary objective is to avoid having near-resonant sites in physical proximity for some specific lattice geometry. Our reasons for this will become clear later. Here, we focus on a quasi-one-dimensional (1D) square lattice with dimensions $2 \times L$, such as the one depicted in Fig. 1. Such a lattice geometry is already in use for actual quantum computing devices [17] and may also become even more relevant for future designs. Using integer-valued real-space coordinates (x_i, y_i) for site i, where y is the short axis and x the long axis of length $L > 2$, we introduce the disorder potential:

$$\omega_i = \langle\omega\rangle + \Delta\sqrt{2}\sin\left[\pi x_i\left(y_i + \sqrt{y_i^2 + 4}\right)\right]. \qquad (5)$$

Here, $\langle\omega\rangle$ is the central value around which the transmon frequencies vary with a strength that is determined by the sine function amplitude Δ. More precisely, the parameter definitions have been chosen such that, in the thermodynamic limit

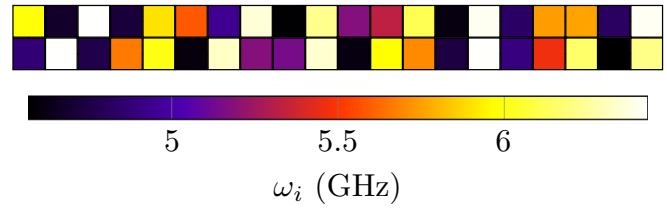

FIG. 1. Metallic Aubry-André disorder potential: Transmon frequency disorder potential $\omega(x_i, y_i)$ [Eq. (5)] for a quasi-one-dimensional (1D) lattice of dimensions 2×20. We use mean frequency $\langle\omega\rangle = 5.5$ GHz and disorder strength $\Delta = 1$ GHz. The on-site frequencies are color coded according to the given color bar and the values are given in GHz. The bottom row of the lattice corresponds to $y = 1$ and the top to $y = 2$. The leftmost sites of the lattice have $x = 1$ and the rightmost $x = 20$.

$(N \to \infty)$, we will have

$$\frac{1}{N}\sum_{i=1}^{N} \omega_i \to \langle\omega\rangle \quad \text{and} \quad \sqrt{\frac{1}{N}\sum_{i=1}^{N} (\omega_i - \langle\omega\rangle)^2} \to \Delta. \qquad (6)$$

In other words, $\langle\omega\rangle$ is the average and Δ the standard deviation.

The inspiration behind using this potential is the Aubry-André model commonly used in the study of 1D quasicrystals, where it exhibits a well-studied transition between Anderson localized [18,19] and delocalized phases [20–24]. As a matter of fact, treating the y coordinate as a fixed parameter, we recover the exact form of the Aubry-André model. Simply put, along the x direction, the disorder potential is Aubry-André, while changing the y coordinate simply changes the period of the sine function. For the potential to be nonperiodic, the periodicity of the sine function must be chosen so that it is incommensurate with the integer periodicity of the lattice. This is done here by making the periodicity irrational, and since we need the periodicity to be varying with y, we need a family of irrational numbers, hence our choice of the metallic ratios [25].

With the metallic Aubry-André (MAA) model as our choice of the disorder potential, our first goal is to establish how well it performs in localizing our system compared with random disorder. We have first performed this comparison for a small system of size 2×3, which is manageable with exact diagonalization. The results are reported in Fig. 2 and confirm that our model outperforms random disorder of the same strength.

A. Perturbation in the anharmonicity

Using the Hamiltonian in Eq. (4) as an effective description of our system, we will obtain the Walsh-Hadamard coefficients perturbatively in the anharmonicity. All the results that will be presented in this section are derived in Appendix A. The first two terms of the Hamiltonian in Eq. (4) describe the *noninteracting* part of the Hamiltonian. We call it noninteracting in the sense that, since it is quadratic in the ladder operators, in the eigenbasis, it should obtain the form of uncoupled harmonic oscillators. In the *bare basis*, the noninteracting part of the Hamiltonian is, however, not diagonal, and to use perturbation theory, we first need to transform the

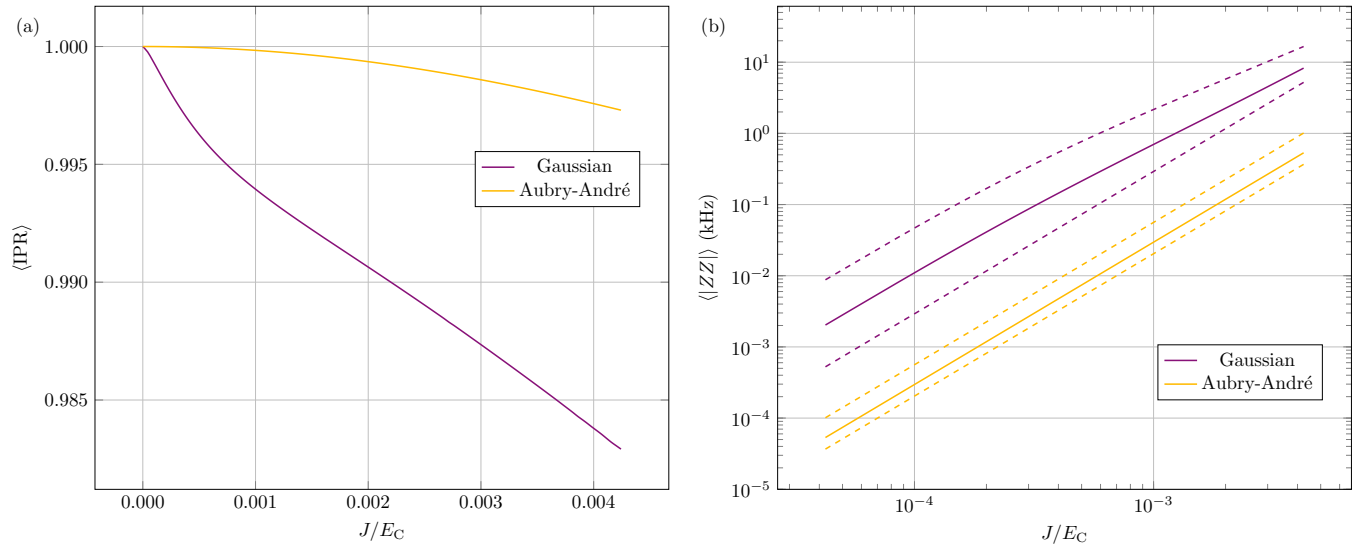

FIG. 2. Random Gaussian disorder vs metallic Aubry-André (MAA): Exact diagonalization results for averaged (a) inverse participation ratio (IPR) and (b) Walsh-Hadamard coefficients as a function of the hopping strength J in units of the anharmonicity E_C for MAA and random Gaussian disorder with matching standard deviation. The averaging is done over (a) all eigenstates and (b) Walsh-Hadamard coefficients of weight 2 and correlation range $\ell = 1$ (nearest-neighbor ZZ coefficients). Particularly for the ZZ coefficients plot, the dashed lines indicate the range of the ZZ coefficients of the solid line with the same color. For the case of the Gaussian random disorder, there is additional averaging over 100 different realizations. The parameter values used here are $E_C = 0.33$ GHz, $\langle\omega\rangle = 5.5$ GHz, and $\Delta = 1$ GHz, and the coupling J is varied over the range 0–1.5 MHz. The system size for both cases is 2×3.

Hamiltonian to the *dressed basis* defined by the relation:

$$c_\mu^\dagger|0\rangle \stackrel{!}{=} \left[\sum_{i=1}^{N} \psi_\mu(x_i, y_i) a_i^\dagger\right]|0\rangle, \tag{7}$$

where $c_\mu^\dagger$ creates a single-excitation eigenstate $|\psi_\mu\rangle$ of the noninteracting Hamiltonian. For clarity, we reserve Latin indices for the bare basis and Greek indices for the dressed basis.

Since we are only interested in the localized regime of the system, we could perform the transformation of Eq. (7) perturbatively as well (in the coupling J). However, this adds one additional layer of complexity to our final expressions, without leading to any particular new insights. Therefore, we choose to obtain the single-particle sector spectrum numerically and use these results as input to our derived analytic expressions from second-order perturbation theory in the anharmonicity E_C.

In the dressed basis, our Hamiltonian is recast into the form:

$$H_{\mathrm{DBH}} = \sum_{\mu=1}^{N} \varepsilon_\mu c_\mu^\dagger c_\mu - \frac{E_C}{2} \sum_{\alpha,\beta,\mu,\nu=1}^{N} V_{\alpha\beta\mu\nu} c_\alpha^\dagger c_\beta^\dagger c_\mu c_\nu, \tag{8}$$

where ε_μ is the energy of a single excitation on site μ of the noninteracting Hamiltonian, and we have also defined the 4-point correlation tensor:

$$V_{\alpha\beta\mu\nu} = \sum_{i=1}^{N} \psi_\alpha(x_i, y_i)\psi_\beta(x_i, y_i)\psi_\mu(x_i, y_i)\psi_\nu(x_i, y_i), \tag{9}$$

and we have made explicit use of the fact that our eigenstates are real. For sufficiently weak transmon coupling J, the single-excitation eigenstates should be exponentially localized around lattice site μ with coordinates (x_μ, y_μ), and the dressed basis should be nearly identical to the bare basis $c_\mu^\dagger \approx a_\mu^\dagger$ and by extension for the energy levels as well: $\varepsilon_\mu \approx \omega_\mu$. Therefore, even though the capacitive energy E_C is not the smallest energy scale in our system, the use of perturbation theory is justified if we are in the transmon regime since $E_C/\varepsilon_\mu \approx E_C/\omega_\mu \sim \sqrt{E_C/E_{J_\mu}} \ll 1$.

For the Walsh-Hadamard coefficients of Eq. (2), we only need to obtain the perturbed energy levels that correspond to qubit states:

$$|b\rangle = \prod_{\mu=1}^{N} (c_\mu^\dagger)^{b_\mu}|0\rangle, \tag{10}$$

where b_μ is the μth binary digit of bit-string b. By allowing the bit-string digits to be undetermined parameters of possible value 0 or 1, we can obtain the energy correction for an arbitrary qubit state of any N-transmon array. The only thing that we need to calculate the involved amplitudes in the perturbation theory are the generalized Wick contraction rules for operators with binary undetermined exponents given by

$$\overbrace{c_\mu^{b_\alpha}(c_\nu^\dagger)^{b_\beta}} = \delta_{\mu\nu}\delta_{b_\alpha,b_\beta}, \tag{11}$$

while all other possible contractions are vanishing. It is straightforward to convince oneself of the validity of this relation simply by considering all four possible combinations of values for b_α and b_β. With these rules in hand, the relevant amplitudes can be calculated inductively using the method described in Ref. [26]. See Appendixes A 1 and A 2 for an analytic derivation of these results.

Due to the linearity of the Walsh-Hadamard transformation, we can apply it separately at each order of perturbation

theory for the qubit-sector energy levels, yielding a series expansion for the Walsh-Hadamard coefficients themselves:

$$w_b = w_b^{(0)} + w_b^{(1)} + w_b^{(2)} + \cdots . \tag{12}$$

Furthermore, the analytical expressions for the energy levels contain terms that are proportional to products of a few bit-digits, particularly up to 3-digit products for the second order in perturbation theory that we calculated here. Such m-digit products transform like

$$\begin{aligned}\Pi_{\mu_1\mu_2\ldots\mu_m}(b) &= \frac{1}{2^N}\sum_{a\in\mathbb{B}^N}(-1)^{b\cdot\bar{a}}a_{\mu_1}a_{\mu_2}\ldots a_{\mu_m}\\ &= \frac{1}{2^m}\prod_{i\neq\mu_1,\mu_2,\ldots,\mu_m}\bar{b}_i.\end{aligned} \tag{13}$$

From Eq. (13), it becomes apparent that, if the Walsh-Hadamard coefficient corresponds to a bit-string b of weight more than m, then $\Pi_{\mu_1\ldots\mu_m}(b) = 0$. As a direct consequence of this, first-order perturbation theory can only yield corrections for Walsh-Hadamard coefficients up to weight 2 and second-order perturbation theory up to weight 3 (see Appendix A 3 for more details). The exact form of these coefficients is

$$w_b^{(0)} = \sum_\mu \varepsilon_\mu \Pi_\mu(b), \tag{14a}$$

$$w_b^{(1)} = \sum_{\mu<\nu} \mathcal{E}_{\mu\nu}\Pi_{\mu\nu}(b), \tag{14b}$$

$$w_b^{(2)} = \sum_{\substack{\mu<\nu\\ \alpha,\beta}} \mathcal{D}_{\mu\nu\alpha\beta}\Pi_{\mu\nu}(b) + \sum_{\substack{\mu<\nu<\alpha\\ \beta}} \mathcal{S}_{\mu\nu\alpha\beta}\Pi_{\mu\nu\alpha}(b), \tag{14c}$$

where we have used the tensor definitions:

$$\mathcal{E}_{\mu\nu} = 2E_C V_{\mu\mu\nu\nu}, \tag{15a}$$

$$\mathcal{D}_{\mu\nu\alpha\beta} = \frac{E_C^2}{2}\frac{|V_{\mu\nu\alpha\beta}|^2}{\varepsilon_\mu+\varepsilon_\nu-\varepsilon_\alpha-\varepsilon_\beta}, \tag{15b}$$

$$\mathcal{J}_{\mu\nu\alpha\beta} = E_C^2\frac{V_{\mu\mu\alpha\beta}V_{\nu\nu\alpha\beta}}{\varepsilon_\alpha-\varepsilon_\beta}, \tag{15c}$$

$$\mathcal{S}_{\mu\nu\alpha\beta} = 4![\mathcal{D}_{(\mu\nu\alpha)\beta} + \mathcal{J}_{(\mu\nu\alpha)\beta}]. \tag{15d}$$

The instances which are divergent according to these definitions, $\mathcal{D}_{\mu\nu\mu\nu}, \mathcal{D}_{\mu\nu\nu\mu}$, and $\mathcal{J}_{\mu\nu\alpha\alpha}$, do not appear in the expressions for w_b. We have also used the notation for the fully symmetric component of a tensor T with respect to the indices in parentheses, which for our case simplifies due to the explicit symmetry of our tensors $\mathcal{D}$ and $\mathcal{J}$ with respect to the first two indices to

$$T_{(\mu\nu\alpha)\beta} = \tfrac{1}{3}(T_{\mu\nu\alpha\beta} + T_{\mu\alpha\nu\beta} + T_{\nu\alpha\mu\beta}). \tag{16}$$

By using the MAA scheme, we set up a quasirandom disorder potential without resonances and with well-separated near-resonant sites. While the four-term denominator of $\mathcal{D}$ creates some dangers for perturbation theory, its numerators have a counteracting effect. They are proportional to the 4-point function $V_{\mu\nu\alpha\beta}$ of the single-particle eigenvectors involving the same states as the ones in the denominator. Anderson localization theory ensures that these correlations decay exponentially with range.

With this perturbation theory, we can move on to obtain Walsh-Hadamard coefficients for a much larger system of dimensions 2×20. Before doing that, however, we examine the accuracy of our perturbation theory by comparing it with exact diagonalization results. For this comparison, still restricted to the 2×3 system size, see Fig. 3. It is evident that the agreement of the two results is restricted to a rather small parameter range. Even though the second-order perturbation theory is very accurate for the energy levels, with an error of $\sim 10^{-1}$ kHz for eigenenergies spanning a few tens of GHz, the error is of the same order of magnitude as the Walsh-Hadamard coefficients of weight 2 and is $\sim$2 orders of magnitude larger than coefficients of weight 3. This is why we only report the weight-2 coefficients here. Unfortunately, the accuracy of the energy levels is not found to be improved by introducing higher-order terms [27]; our perturbation theory is equivalent to that of the φ^4 theory, which is known to have a vanishing radius of convergence. Already at third order of perturbation theory, the disagreement with the exact diagonalization results starts to increase.

Despite these difficulties, we obtain meaningful results for the Walsh-Hadamard coefficients and the correct order of magnitude within the parameter range $\Delta \gtrsim 4E_C$, as can be seen in Fig. 3. Therefore, we proceed to obtain the weight-2 coefficients using perturbation theory for the much larger 2×20 system, beyond the size that is easily accessible to exact diagonalization. The results for this calculation are reported in Fig. 4. They confirm the expectation that these Walsh-Hadamard coefficients exhibit a strong hierarchy of values, decreasing exponentially with range; this is as expected within MBL theory (see Ref. [9]).

B. Perturbation in the hopping strength

We have seen that treating the many-body interactions perturbatively yields information for the MBL of the system but only for extremely weak anharmonicity or strong disorder. To overcome this restricted radius of convergence, we need to employ a different perturbative scheme without the pathologies of the φ^4 theory. Here, we will treat perturbatively instead the hopping strength J of the system Hamiltonian in Eq. (4).

For this scheme, the unperturbed Hamiltonian is diagonal in the bare basis with qubit states represented by

$$|b\rangle = \prod_{\mu=1}^{N}(a_\mu^\dagger)^{b_\mu}|0\rangle, \tag{17}$$

and therefore, we can apply immediately RS perturbation theory without going to the dressed basis. We again perform a second-order perturbation theory calculation for the qubit-sector energy levels (see Appendix B for derivation) and apply the Walsh-Hadamard transformation on the analytic expressions for the energy levels to derive the following results:

$$w_b^{(0)} = \sum_j \omega_j \Pi_j(b), \tag{18a}$$

$$w_b^{(1)} = 0, \tag{18b}$$

$$w_b^{(2)} = J^2\sum_{\langle i<j\rangle}\left[\frac{4E_C}{E_C^2-\delta_{ij}^2} + \frac{2(b_i-b_j)}{\delta_{ij}}\right]\Pi_{ij}(b), \tag{18c}$$

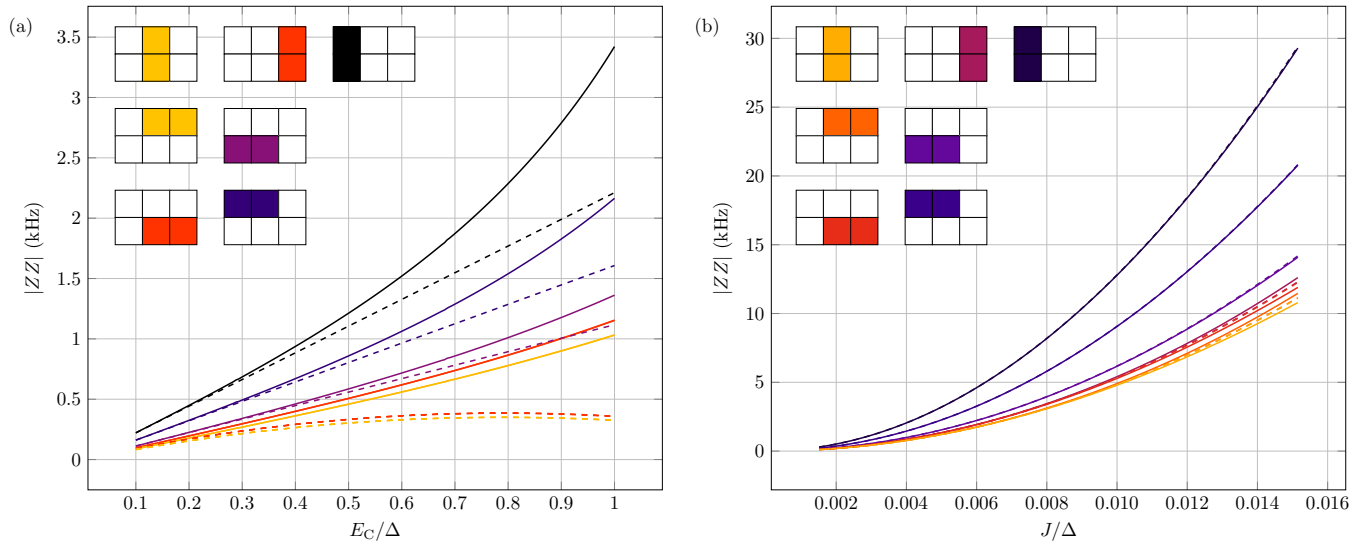

FIG. 3. Exact diagonalization vs perturbation theory for the metallic Aubry-André model: Plots of all the nearest-neighbor ZZ coefficients as a function of (a) the small parameter E_C and (b) J, expressed in units of disorder strength Δ. Exact diagonalization results are represented by solid lines and perturbation theory with dashed lines. The parameter values used for (a) are $\Delta = 1$ GHz and $J = 2.5$ MHz, and the anharmonicity E_C is varied over the range 0.1Δ to Δ. In (b) are $E_C = 0.33$ GHz and $\Delta = 2E_C$, and the hopping strength J is varied over the range 1–10 MHz. For both cases, $\langle\omega\rangle = 5.5$ GHz, and the system size is 2×3. Coefficients are color coded with respect to the corresponding site pair, see legend.

where we have defined the detuning between sites i and j as $\delta_{ij} = \omega_i - \omega_j$. With the bracketed summation indices $\langle i < j \rangle$, we denote summation with respect to the indices i and j of nearest-neighbor sites only and with a fixed ordering

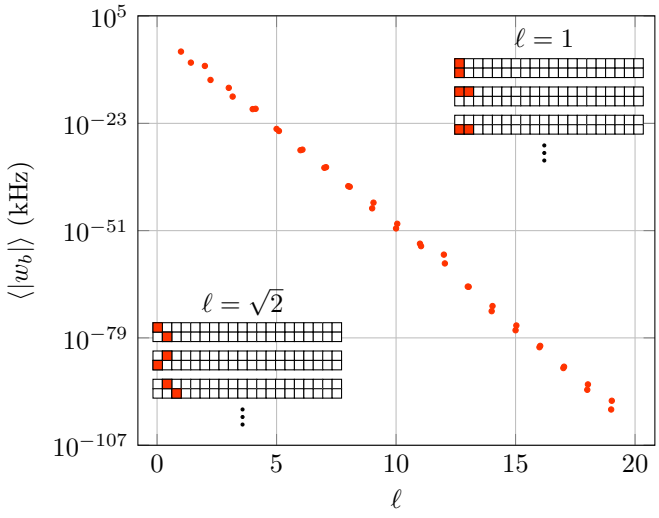

FIG. 4. Exponential hierarchy of the Walsh-Hadamard coefficients for the metallic Aubry-André model: Plot of averaged Walsh-Hadamard coefficients of weight 2 as a function of the correlation range ℓ for a 2×20 quasi-one-dimensional (1D) lattice. Averaging is done among Walsh-Hadamard coefficients of the same correlation range. The parameter values used here are $J = 1$ MHz, $\langle\omega\rangle = 5.5$ GHz, $E_C = 0.33$ GHz, and $\Delta = 3E_C$. The inset is a visual representation of the relevant Walsh-Hadamard coefficient bit strings for correlation ranges $\ell = 1$ and $\sqrt{2}$ on the lattice. Filled boxes represent excited sites, while empty ones represent the ground state.

to avoid double counting pairs. The bit-digit products $\Pi_j(b)$ and $\Pi_{ij}(b)$ are the ones already defined in Eq. (13).

In Fig. 3(b), we present a comparison of the perturbation theory results of Eqs. (18a)–(18c) with the numerical values of the Walsh-Hadamard coefficients obtained with exact diagonalization for a small system of dimensions 2×3. The RS perturbation scheme is strikingly accurate, especially when compared with the accuracy of the MP result in Fig. 3(a). Even more remarkably, the RS perturbation theory scheme manages to capture the features of our model significantly further away from the strongly localized regime. This is evident from the fact that, within the presented range of J values, the ZZ coefficients have managed to climb to values an order of magnitude higher than the corresponding case for MP perturbation theory, with virtually no drop in accuracy.

This drastic improvement in accuracy with our perturbation theory scheme, however, comes at the cost of a reduced capability of probing the exponential hierarchy of the Walsh-Hadamard coefficients. Note that, up to second order in perturbation theory, we can only obtain corrections for bit-strings of up to weight 2 using the same argument given right after the definition of the bit-digit products in Eq. (13). Additionally, the summation in Eq. (18c) is over nearest-neighbour pairs only. From the last two observations, we can infer that only ZZ coefficients can be estimated with second-order perturbation theory. Even for weight-2 bit-strings of longer correlation range $\ell > 1$, we would need to go to higher orders of perturbation theory.

However, another advantage of the RS perturbation scheme is the significantly lower computational cost for obtaining the ZZ coefficients. According to Eq. (18c), calculating a particular ZZ coefficient to second order, one needs to only calculate a single term for i, j, referring to the sites of the

ZZ coefficient under consideration. In contrast, using the MP perturbation scheme for the second-order ZZ coefficients, one needs to invoke a summation of $\sim N^2$ terms. As a result, we can calculate the second-order ZZ coefficients for a system size of 2×2000 in a matter of seconds using the RS scheme, while MP requires several minutes to yield the same results for a 2×20 system like the one presented in Fig. 4.

III. CONCLUSIONS

We have demonstrated that it is possible to localize a many-body quantum computing system without the use of random disorder but rather with a deterministically designed, non-periodic potential. We believe that the disorder potential we studied here is not yet optimal and that meticulous frequency pattern engineering should play a crucial role in the design of future quantum computing architectures. Our perturbation-theory scheme can be used as a guide for the properties a frequency pattern should possess or avoid. Despite the limited accuracy of the MP perturbation scheme, we have demonstrated that it is possible to obtain useful analytical results for the Walsh-Hadamard coefficients of large many-body systems. We believe that accuracy can ultimately be improved with a renormalized perturbation theory in the anharmonicity. Finally, we need to stress that the results for the 2×20 lattice are beyond the realm of what is attainable with exact diagonalization techniques and of course the 2×2000 lattice even far more so. The main impediment for increasing the size further is the exponential scaling of the number of Walsh-Hadamard coefficients themselves, which is 2^N. However, if we instead restrict the calculation to only low-weight coefficients with small correlation range, then we can obtain reliable results using the RS scheme for extremely large systems, without any compromise in accuracy, if we remain in the desired localized regime.

ACKNOWLEDGMENTS

We acknowledge support from the Deutsche Forschungsgemeinschaft (DFG) under Germany's Excellence Strategy Cluster of Excellence Matter and Light for Quantum Computing (ML4Q) EXC 2004/1 390534769.

APPENDIX A: MP PERTURBATION THEORY

We start with a Hamiltonian of the form given in Eq. (8) but without making any assumption for the form of the tensor $V_{\alpha\beta\mu\nu}$, except that it is real. However, there are two symmetries that will simplify our calculation significantly without loss of generality. The first one is the fact that

$$\sum_{\alpha,\beta,\mu,\nu} V_{\alpha\beta\mu\nu} c_\alpha^\dagger c_\beta^\dagger c_\mu c_\nu = \sum_{\alpha,\beta,\mu,\nu} V_{\alpha\beta\mu\nu} c_\beta^\dagger c_\alpha^\dagger c_\mu c_\nu = \sum_{\alpha,\beta,\mu,\nu} V_{\beta\alpha\mu\nu} c_\alpha^\dagger c_\beta^\dagger c_\mu c_\nu, \quad \text{(A1)}$$

where in the first step, we used the commutativity of the bosonic operators, and in the second step, we performed a summation index relabeling. Even though this property does not guarantee that $V_{\alpha\beta\mu\nu} = V_{\beta\alpha\mu\nu}$, it does suggest that, if $V_{\alpha\beta\mu\nu}$ has an antisymmetric component with respect to the first two indices, then that component yields no contribution to the sum. Since we can always decompose $V_{\alpha\beta\mu\nu}$ to symmetric and antisymetric components, it means we can assume without loss of generality that $V_{\alpha\beta\mu\nu}$ can always be symmetrized with respect to the first two indices without changing the Hamiltonian of the system. The same argument can be made for the last two indices. The second argument follows along similar lines:

$$\sum_{\alpha,\beta,\mu,\nu} V_{\alpha\beta\mu\nu} c_\alpha^\dagger c_\beta^\dagger c_\mu c_\nu = \sum_{\alpha,\beta,\mu,\nu} V_{\alpha\beta\mu\nu} c_\nu^\dagger c_\mu^\dagger c_\beta c_\alpha = \sum_{\alpha,\beta,\mu,\nu} V_{\mu\nu\alpha\beta} c_\alpha^\dagger c_\beta^\dagger c_\mu c_\nu, \quad \text{(A2)}$$

where in the first step, we used the hermiticity of the sum, and in the second step, we performed a summation index relabeling. Once again, this does not imply $V_{\alpha\beta\mu\nu} = V_{\mu\nu\alpha\beta}$; however, any component antihermitian with respect to the index pair exchange would have vanishing contribution to the sum, and hence, $V_{\alpha\beta\mu\nu}$ can be thought as symmetric with respect to the index pair exchange without loss of generality. In summary, our symmetries for the tensor are

$$V_{\alpha\beta\mu\nu} = V_{\beta\alpha\mu\nu} = V_{\alpha\beta\nu\mu} = V_{\mu\nu\alpha\beta}. \quad \text{(A3)}$$

The tensor for the system we study in the main text has more symmetries than these, and therefore, what we present here is a more generic case.

Since the ladder operators are bosonic, the system has an infinite number of eigenstates. However, for the Walsh-Hadamard coefficients, we are only interested in the finite subspace of qubit states of Eq. (10). For this family of states, the unperturbed energy levels take the form:

$$E_b^{(0)} = \langle b|H_0|b\rangle = \sum_\mu E_\mu b_\mu, \quad \text{(A4)}$$

and starting with this, we can now obtain the energy levels of the generalized Hamiltonian with the usual RS perturbation theory.

1. First-order energy correction

At first order in perturbation theory, we will have

$$E_b^{(1)} = \sum_{\alpha,\beta,\mu,\nu} V_{\alpha\beta\mu\nu} \langle b|c_\alpha^\dagger c_\beta^\dagger c_\mu c_\nu|b\rangle. \quad \text{(A5)}$$

If we substitute the state of Eq. (10) in this definition, the calculation of the first-order correction boils down to a single vacuum expectation value, which in turn can be evaluated by means of Wick contractions according to the rules presented in Eq. (11). To do this, we need to fully contract the operators. We will do this using the permanent method described in Ref. [26], which consists of calculating the permanent of the

matrix whose elements corresponding to all possible Wick contractions between an annihilation operator, corresponding to a row, and a creation operator, corresponding to a column. Using the basis $\{c_\mu, c_\nu, c_1^{b_1}, \ldots, c_N^{b_N}\}$ for the rows and $\{c_\alpha^\dagger, c_\beta^\dagger, (c_1^\dagger)^{b_1}, \ldots, (c_N^\dagger)^{b_N}\}$ for the columns, we can write Eq. (11) in matrix form:

$$\mathcal{C}_{\alpha\beta\mu\nu}(b) = \begin{pmatrix} 0 & 0 & b_1\delta_{\mu,1} & \ldots & b_N\delta_{\mu,N} \\ 0 & 0 & b_1\delta_{\nu,1} & \ldots & b_N\delta_{\nu,N} \\ b_1\delta_{\alpha,1} & b_1\delta_{\beta,1} & 1 & \ldots & 0 \\ \vdots & \vdots & \vdots & \ddots & \vdots \\ b_N\delta_{\alpha,N} & b_N\delta_{\beta,N} & 0 & \ldots & 1 \end{pmatrix}. \tag{A6}$$

For the first-order correction, we will have from Eq. (A5)

$$E_b^{(1)} = \sum_{\alpha,\beta,\mu,\nu} V_{\alpha\beta\mu\nu}\,\mathrm{perm}[\mathcal{C}_{\alpha\beta\mu\nu}(b)]. \tag{A7}$$

By definition, the permanent of a $d \times d$ matrix is the sum over all possible products consisted of d elements of the matrix with no two of them sharing a row or column. From the first two rows, only elements past column 2 have a nonvanishing contribution to the product; therefore, for example, if we select elements $2+\rho$ and $2+\sigma$ from the first and second rows, respectively, we will have a factor of $b_\rho b_\sigma \delta_{\mu\rho}\delta_{\nu\sigma}$ with the restriction that $\rho \neq \sigma$, which can be enforced by multiplying this expression with $|\varepsilon_{\rho\sigma}|$, with ε denoting the fully antisymmetric tensor. Having selected an element from columns $2+\rho$ and $2+\sigma$ means that we have effectively removed these entire columns, and therefore, at the corresponding rows, the only possible choices that lead to a nonvanishing contribution are from columns 1 and 2, yielding either $b_\rho b_\sigma \delta_{\alpha\rho}\delta_{\beta\sigma}$ or $b_\rho b_\sigma \delta_{\alpha\sigma}\delta_{\beta\rho}$. With the first two rows and columns of the matrix removed, we can only choose elements from the identity matrix at the bottom right of the contraction matrix. The permanent for our two-body interaction case yields

$$E_b^{(1)} = \sum_{\substack{\alpha,\beta,\mu,\nu \\ \rho,\sigma}} V_{\alpha\beta\mu\nu} b_\rho b_\sigma |\varepsilon_{\rho\sigma}| \delta_{\mu\rho}\delta_{\nu\sigma}(\delta_{\alpha\rho}\delta_{\beta\sigma} + \delta_{\alpha\sigma}\delta_{\beta\rho}). \tag{A8}$$

Performing the summation with respect to ρ, σ, α, and β and using the symmetries of the interaction potential Eq. (A3), we obtain

$$E_b^{(1)} = \sum_{\mu<\nu} \mathcal{E}_{\mu\nu} b_\mu b_\nu, \tag{A9}$$

where we used the tensor definition:

$$\mathcal{E}_{\mu\nu} = 4V_{\mu\nu\mu\nu}. \tag{A10}$$

Note that, according to the symmetries of $V_{\alpha\beta\mu\nu}$ given in Eq. (A3), the tensor $\mathcal{E}$ should be symmetric:

$$\mathcal{E}_{\mu\nu} = \mathcal{E}_{\nu\mu}. \tag{A11}$$

Finally, performing the Walsh-Hadamard transformation on Eq. (A9), we obtain the result presented in the main text in Eq. (14b). For more details on this, see Appendix A 3.

2. Second-order energy correction

We now proceed with the second-order correction given by

$$E_b^{(2)} = V_{\alpha_1\beta_1\mu_1\nu_1} V_{\alpha_2\beta_2\mu_2\nu_2} \times \sum_{m\neq b} \frac{\langle b|c_{\alpha_1}^\dagger c_{\beta_1}^\dagger c_{\mu_1} c_{\nu_1}|m\rangle\langle m|c_{\alpha_2}^\dagger c_{\beta_2}^\dagger c_{\mu_2} c_{\nu_2}|b\rangle}{E_b^{(0)} - E_m^{(0)}}, \tag{A12}$$

where we have used the Einstein summation convention here to lighten the notation. We have a new complication here since the eigenstates $|m\rangle$ of the free Hamiltonian are not necessarily qubit states anymore, and as a result, Wick contraction rules for arbitrary exponents become significantly more complicated. However, we can circumvent this using the following argument. The state resulting from the application of $c_{\alpha_2}^\dagger c_{\beta_2}^\dagger c_{\mu_2} c_{\nu_2}$ on the qubit state $|b\rangle$ is still an eigenstate $|n_2\rangle$ of the free Hamiltonian, although it might not be normalized anymore:

$$c_{\alpha_2}^\dagger c_{\beta_2}^\dagger c_{\mu_2} c_{\nu_2}|b\rangle = \lambda_2|n_2\rangle. \tag{A13}$$

A similar argument follows for the bracket:

$$\langle b|c_{\alpha_1}^\dagger c_{\beta_1}^\dagger c_{\mu_1} c_{\nu_1} = \lambda_1\langle n_1|, \tag{A14}$$

and therefore, we can write using Eq. (A12)

$$\begin{aligned} E_b^{(2)} &= \lambda_1\lambda_2 V_{\alpha_1\beta_1\mu_1\nu_1} V_{\alpha_2\beta_2\mu_2\nu_2} \sum_{m\neq b} \frac{\langle n_1|m\rangle\langle m|n_2\rangle}{E_b^{(0)} - E_m^{(0)}} \\ &= \lambda_1\lambda_2 V_{\alpha_1\beta_1\mu_1\nu_1} V_{\alpha_2\beta_2\mu_2\nu_2} \sum_{m\neq b} \frac{\delta_{n_1,m}\delta_{n_2,m}}{E_b^{(0)} - E_m^{(0)}} \\ &= \lambda_1\lambda_2 V_{\alpha_1\beta_1\mu_1\nu_1} V_{\alpha_2\beta_2\mu_2\nu_2} \frac{\delta_{n_1,n_2}}{E_b^{(0)} - E_{n_2}^{(0)}}\bigg|_{n_2\neq b} \\ &= V_{\alpha_1\beta_1\mu_1\nu_1} V_{\alpha_2\beta_2\mu_2\nu_2} \frac{\lambda_1\lambda_2\langle n_1|n_2\rangle}{E_b^{(0)} - E_{n_2}^{(0)}}\bigg|_{n_2\neq b}. \end{aligned} \tag{A15}$$

Finally, since by definition the state $|n_2\rangle$ is obtained from $|b\rangle$ by extracting two excitations from sites μ_2 and ν_2 and adding two at sites α_2 and β_2, we will have

$$E_{n_2} = E_b - \varepsilon_{\mu_2} - \varepsilon_{\nu_2} + \varepsilon_{\alpha_2} + \varepsilon_{\beta_2}, \tag{A16}$$

and in total:

$$E_b^{(2)} = V_{\alpha_1\beta_1\mu_1\nu_1} V_{\alpha_2\beta_2\mu_2\nu_2} \times \frac{\langle b|c_{\alpha_1}^\dagger c_{\beta_1}^\dagger c_{\mu_1} c_{\nu_1} c_{\alpha_2}^\dagger c_{\beta_2}^\dagger c_{\mu_2} c_{\nu_2}|b\rangle}{\varepsilon_{\mu_2} + \varepsilon_{\nu_2} - \varepsilon_{\alpha_2} - \varepsilon_{\beta_2}}\bigg|_{\{\alpha_2,\beta_2\}\neq\{\mu_2,\nu_2\}}, \tag{A17}$$

where $\{\alpha_2, \beta_2\} \neq \{\mu_2, \nu_2\}$ is meant in the sense of set inequality. Once again, we have an amplitude involving only a single qubit state, and therefore, we can use the Wick rules from the first-order calculation, leading directly to the

contraction matrix:

$$\begin{pmatrix} 0 & 0 & \delta_{\mu_1\alpha_2} & \delta_{\mu_1\beta_2} & b_1\delta_{\mu_1,1} & \dots & b_N\delta_{\mu_1,N} \\ 0 & 0 & \delta_{\nu_1\alpha_2} & \delta_{\nu_1\beta_2} & b_1\delta_{\nu_1,1} & \dots & b_N\delta_{\nu_1,N} \\ 0 & 0 & 0 & 0 & b_1\delta_{\mu_2,1} & \dots & b_N\delta_{\mu_2,N} \\ 0 & 0 & 0 & 0 & b_1\delta_{\nu_2,1} & \dots & b_N\delta_{\nu_2,N} \\ b_1\delta_{\alpha_1,1} & b_1\delta_{\beta_1,1} & b_1\delta_{\alpha_2,1} & b_1\delta_{\beta_2,1} & 1 & \dots & 0 \\ \vdots & \vdots & \vdots & \vdots & \vdots & \ddots & \vdots \\ b_N\delta_{\alpha_1,N} & b_N\delta_{\beta_1,N} & b_N\delta_{\alpha_2,N} & b_N\delta_{\beta_2,N} & 0 & \dots & 1 \end{pmatrix}. \tag{A18}$$

For this case, since the effective four-body interaction is not normally ordered already, we have additional contractions. There are multiple ways to deal with this, namely, normally ordering the interaction term using the bosonic algebra, the method of reduced permanents, or considering cases as we did before for the first-order correction. The results are summarized in the following expression:

$$E_b^{(2)} = \sum_{\substack{\alpha<\beta \\ \mu,\nu}} \mathcal{D}_{\alpha\beta\mu\nu} b_\alpha b_\beta + \sum_{\substack{\alpha<\beta<\mu \\ \nu}} \mathcal{S}_{\alpha\beta\mu\nu} b_\alpha b_\beta b_\mu, \tag{A19}$$

where we have also introduced the tensor definitions:

$$\mathcal{D}_{\alpha\beta\mu\nu} = \begin{cases} \dfrac{2|V_{\alpha\beta\mu\nu}|^2}{\varepsilon_\alpha + \varepsilon_\beta - \varepsilon_\mu - \varepsilon_\nu}, & \{\alpha,\beta\} \neq \{\mu,\nu\}, \\ 0, & \{\alpha,\beta\} = \{\mu,\nu\}, \end{cases} \tag{A20a}$$

$$\mathcal{J}_{\alpha\beta\mu\nu} = \begin{cases} \dfrac{4V_{\alpha\mu\alpha\nu}V_{\beta\mu\beta\nu}}{\varepsilon_\mu - \varepsilon_\nu}, & \mu \neq \nu, \\ 0, & \mu = \nu, \end{cases} \tag{A20b}$$

$$\mathcal{S}_{\alpha\beta\mu\nu} = 4![\mathcal{D}_{(\alpha\beta\mu)\nu} + \mathcal{J}_{(\alpha\beta\mu)\nu}], \tag{A20c}$$

with the indices in parentheses denoting the symmetrization of Eq. (16) in the main text. In conjunction with Eq. (A3), we can conclude the following symmetries:

$$\mathcal{D}_{\alpha\beta\mu\nu} = \mathcal{D}_{\beta\alpha\mu\nu} = \mathcal{D}_{\alpha\beta\nu\mu} = -\mathcal{D}_{\mu\nu\alpha\beta}, \tag{A21}$$

$$\mathcal{J}_{\alpha\beta\mu\nu} = \mathcal{J}_{\beta\alpha\mu\nu} = -\mathcal{J}_{\alpha\beta\nu\mu}, \tag{A22}$$

and $\mathcal{S}_{\mu\nu\alpha\beta}$ is symmetric under any permutation of the first three indices.

The antisymmetric property of the tensors $\mathcal{D}$ and $\mathcal{J}$ is the reason why, in the second-order correction of Eq. (A19), we have no four-bit terms. Indeed, Eq. (A19) is the result of the summation over all possible full contractions of the amplitude in Eq. (A17). For the final step, we once again apply the Walsh-Hadamard transformation on Eq. (A19) to obtain the result of the main text presented in Eq. (14c). We will give more details on this in the following section.

3. Second-order Walsh-Hadamard coefficients

With the RS perturbation theory results of Eqs. (A9) and (A19) for the qubit state energy levels, we can now derive the Walsh-Hadamard coefficients via direct application of the definition in Eq. (2). Furthermore, since the transformation is linear, we can perform it term by term:

$$w_b^{(n)} = \frac{1}{2^N} \sum_{q\in\mathbb{B}^N} (-1)^{b\cdot\bar{q}} E_q^{(n)}. \tag{A23}$$

We start with the zeroth-order term of Eq. (A4):

$$w_b^{(0)} = \frac{1}{2^N} \sum_{\mu=1}^{N} \sum_{q\in\mathbb{B}^N} (-1)^{b\cdot\bar{q}} E_\mu q_\mu. \tag{A24}$$

To carry out the Boolean summation, we split the bit-string summation over a product of bit-digit summations and use the following property of functions of binary variables:

$$f(b) = \bar{b} f(0) + b f(1), \tag{A25}$$

from which it follows that

$$\sum_{q=0}^{1} (-1)^{b\bar{q}} = 2\bar{b}, \quad \sum_{q=0}^{1} (-1)^{b\bar{q}} q = 1, \tag{A26}$$

and

$$\sum_{q=0}^{1} (-1)^{b\bar{q}} \bar{q} = 1 - 2b. \tag{A27}$$

As an example, we present the summation explicitly for the zeroth-order case:

$$\begin{aligned} w_b^{(0)} &= \sum_{\mu=1}^{N} \frac{E_\mu}{2^N} \sum_{q\in\mathbb{B}^N} (-1)^{b\cdot\bar{q}} q_\mu \\ &= \sum_{\mu=1}^{N} \frac{E_\mu}{2^N} \left[\prod_{\substack{\rho=1 \\ \rho\neq\mu}}^{N} \sum_{q_\rho=0}^{1} (-1)^{b_\rho\cdot\bar{q}_\rho} \right] \left[\sum_{q_\mu=0}^{1} (-1)^{b_\mu\cdot\bar{q}_\mu} q_\mu \right] \\ &= \sum_{\mu=1}^{N} \frac{E_\mu}{2} \prod_{\substack{\rho=1 \\ \rho\neq\mu}}^{N} \bar{b}_\rho = \sum_{\mu=1}^{N} E_\mu \Pi_\mu(b), \end{aligned} \tag{A28}$$

where in the last step, we used the definition of Eq. (13). For the first- and second-order terms, using the same procedure, we can derive the results presented in Eqs. (14b) and (14c).

The products of the flipped bit-digits pose a sharp cutoff for the weight of Walsh-Hadamard coefficients we can estimate at a finite order of perturbation theory. Namely, for a bit-string $b^{(m)}$ of weight m, the product of all flipped bit-digits excluding k, with $m > k$, will be vanishing for any set of excluded flipped digits since at least one of them will be zero. Therefore, to second order in perturbation theory, we can only obtain corrections for the Walsh-Hadamard coefficients

of weight up to 3. For the nonvanishing cases with $m \leqslant k$, assuming that the nonzero digits of the bit-string are located at positions ℓ_1 through ℓ_m in ascending order, the product will yield one if $\{\ell_1, \ldots, \ell_m\}$ is a subset of the excluded digits. The above can be summarized in the following expression:

$$\Pi_{\mu_1 \ldots \mu_k}[b^{(m)}] = \frac{\theta(k-m)}{2^k} \sum_{s \in [\mu_1, \ldots, \mu_k]^m} \prod_{j=1}^{m} \delta_{\ell_j, s(j)}, \tag{A29}$$

with θ denoting the Heaviside step function with the convention $\theta(0) = 1$, and $[\mu_1, \ldots, \mu_k]^m$ denotes the set of all oriented subsets of length m of the set $\{\mu_1, \ldots, \mu_n\}$. As an example, the flipped digit product for a bit-string of weight $m = 2$ with $k = 3$ excluded digits yields

$$\begin{aligned}\Pi_{\mu_1\mu_2\mu_3}[b^{(2)}] = \tfrac{1}{8}\big(&\delta_{\ell_1}^{\mu_1}\delta_{\ell_2}^{\mu_2} + \delta_{\ell_1}^{\mu_2}\delta_{\ell_2}^{\mu_1} + \delta_{\ell_1}^{\mu_1}\delta_{\ell_2}^{\mu_3} \\ &+ \delta_{\ell_1}^{\mu_3}\delta_{\ell_2}^{\mu_1} + \delta_{\ell_1}^{\mu_2}\delta_{\ell_2}^{\mu_3} + \delta_{\ell_1}^{\mu_3}\delta_{\ell_2}^{\mu_2}\big).\end{aligned} \tag{A30}$$

We used upper indices here only for presentation purposes and no additional context.

APPENDIX B: DERIVATION OF RS PERTURBATION THEORY RESULTS IN THE HOPPING STRENGTH

Starting from the Hamiltonian in Eq. (4) and working in the bare basis, the qubit energy levels to zeroth order in the hopping strength J will be

$$E_b^{(0)} = \sum_{i=1}^{N} \omega_i \langle b|a_i^\dagger a_i|b\rangle = \sum_{i=1}^{N} \omega_i b_i. \tag{B1}$$

Note that contributions from the anharmonicity term are trivially vanishing for qubit states. First-order corrections are also trivially vanishing:

$$E_b^{(1)} = J \sum_{\langle ij \rangle} \langle b|a_i^\dagger a_j|b\rangle = 0. \tag{B2}$$

At second order in perturbation theory, we will have the correction:

$$E_b^{(2)} = J^2 \sum_{m \neq b} \sum_{\substack{\langle ij \rangle \\ \langle k\ell \rangle}} \frac{\langle b|a_k^\dagger a_\ell|m\rangle \langle m|a_i^\dagger a_j|b\rangle}{E_b^{(0)} - E_m^{(0)}}. \tag{B3}$$

We note here that the $|m\rangle$ states are generic bosonic Fock states, and therefore, their unperturbed energy is going to include anharmonic effects:

$$\begin{aligned}E_m^{(0)} &= \sum_{i=1}^{N} \omega_i \langle m|a_i^\dagger a_i|m\rangle - \frac{E_C}{2} \sum_{i=1}^{N} \langle m|a_i^\dagger a_i^\dagger a_i a_i|m\rangle \\ &= \sum_{i=1}^{N} \omega_i m_i - \frac{E_C}{2} \sum_{i=1}^{N} m_i(m_i - 1).\end{aligned} \tag{B4}$$

The numerator of the second-order correction in Eq. (B3) can be calculated using a similar argument as the one we used for the second-order correction of the MP perturbation scheme in Appendix A 2. However, it is more instructive and useful for calculating higher-order corrections to give a diagrammatic interpretation for them as quasiparticles hopping on the lattice.

More precisely, one can interpret the product $\langle b|a_k^\dagger a_\ell|m\rangle \langle m|a_i^\dagger a_j|b\rangle$ as the situation where we start with a configuration of quasiparticles corresponding to the state $|b\rangle$. Since $|b\rangle$ is a qubit state, there is at most one quasiparticle at each side. The first hop occurs by annihilating a quasiparticle at site j and creating it again at an adjacent site i. This first hop brings us to the intermediate state $|m\rangle$ which may or may not be a qubit state. Next, we finish our walk by hopping one quasiparticle from site ℓ to site k which should bring us back to the configuration of state $|b\rangle$. Therefore, the only possible paths are quasiparticles hopping to adjacent sites and then returning to the initial positions:

$$E_b^{(2)} = J^2 \sum_{m \neq b} \sum_{\langle ij \rangle} \frac{\langle b|a_j^\dagger a_i|m\rangle \langle m|a_i^\dagger a_j|b\rangle}{\sum_{k=1}^{N} \omega_k(b_k - m_k) + \frac{E_C}{2} m_k(m_k - 1)}, \tag{B5}$$

where we have also substituted the unperturbed energy levels.

To calculate the weight of each step in this 2-step path, we consider all cases. For the first step, we initially annihilate a quasiparticle at site j, and since the starting state is a qubit state, we will get a factor of $\sqrt{b_j} = b_j$. This last equality is derived from the property of Eq. (A25). We will use this property repeatedly throughout this derivation. Next, we need to create a quasiparticle at the adjacent site i. Since $|b\rangle$ is a qubit state, it is initially at most singly occupied, in which case, we get a factor of $\sqrt{2}$; otherwise, we get a factor of 1. We can summarize this in the factor $2^{b_i/2}$. Note that, with the arrival of the quasiparticle at site j, the state $|m\rangle$ is restricted to have $m_k = b_k$ for all k except from $m_j = 0$ and $m_i = b_i + 1$. For the second step, we start from site i which is now either singly or doubly occupied. With a similar argument as the one we used for the arrival of the quasiparticle at site i, we obtain a factor of $2^{b_i/2}$ for its departure, and since its initial position is certainly empty, the last factor is 1. In total:

$$E_b^{(2)} = J^2 \sum_{\langle ij \rangle} \frac{b_j 2^{b_i}}{\omega_j b_j - \omega_i + \frac{E_C}{2} b_i(b_i + 1)}. \tag{B6}$$

Using the property in Eq. (A25), we can simplify this into

$$E_b^{(2)} = J^2 \sum_{\langle ij \rangle} \left(\frac{\overline{b_i} b_j}{\omega_j - \omega_i} + \frac{2 b_i b_j}{\omega_j - \omega_i + E_C} \right). \tag{B7}$$

As a final step, since every pair of sites i, j appears twice in the sum, we fix an arbitrary order for the summation indices and have

$$E_b^{(2)} = J^2 \sum_{\langle i<j \rangle} \left[\frac{\overline{b_j} b_i - \overline{b_i} b_j}{\omega_i - \omega_j} + \frac{4 b_i b_j E_C}{E_C^2 - (\omega_i - \omega_j)^2} \right]. \tag{B8}$$

Applying the Walsh-Hadamard transformation in Eq. (2) to the expressions that we derived here for the energy corrections and using the properties in Eqs. (A26) and (A27), we can obtain Eqs. (18a)–(18c) of the main text.

The next nonvanishing contribution is at fourth order of perturbation theory. However, in the quasiparticle walks picture that we presented for the second-order calculation, there are now much more ways for the particle to move around, which means we need to consider many different cases, each one contributing a rather complicated summation.

Therefore, presenting this result here does not offer any particular new insights, and for computational purposes, we deem the numerical calculation of the higher-order corrections advantageous, although analytical results are obtainable.

[1] F. Arute, K. Arya, R. Babbush, D. Bacon, J. C. Bardin, R. Barends, R. Biswas, S. Boixo, F. G. Brandao, D. A. Buell *et al.*, Quantum supremacy using a programmable superconducting processor, Nature (London) **574**, 505 (2019).

[2] Y. Wu, W.-S. Bao, S. Cao, F. Chen, M.-C. Chen, X. Chen, T.-H. Chung, H. Deng, Y. Du, D. Fan *et al.*, Strong quantum computational advantage using a superconducting quantum processor, Phys. Rev. Lett. **127**, 180501 (2021).

[3] https://www.ibm.com/quantum-computing/.

[4] L. DiCarlo, J. M. Chow, J. M. Gambetta, L. S. Bishop, B. R. Johnson, D. Schuster, J. Majer, A. Blais, L. Frunzio, S. Girvin *et al.*, Demonstration of two-qubit algorithms with a superconducting quantum processor, Nature (London) **460**, 240 (2009).

[5] F. Yan, P. Krantz, Y. Sung, M. Kjaergaard, D. L. Campbell, T. P. Orlando, S. Gustavsson, and W. D. Oliver, Tunable coupling scheme for implementing high-fidelity two-qubit gates, Phys. Rev. Appl. **10**, 054062 (2018).

[6] J. Ku, X. Xu, M. Brink, D. C. McKay, J. B. Hertzberg, M. H. Ansari, and B. L. T. Plourde, Suppression of unwanted *ZZ* interactions in a hybrid two-qubit system, Phys. Rev. Lett. **125**, 200504 (2020).

[7] X. Xu and M. H. Ansari, *ZZ* freedom in two-qubit gates, Phys. Rev. Appl. **15**, 064074 (2021).

[8] J. B. Hertzberg, E. J. Zhang, S. Rosenblatt, E. Magesan, J. A. Smolin, J.-B. Yau, V. P. Adiga, M. Sandberg, M. Brink, J. M. Chow *et al.*, Laser-annealing Josephson junctions for yielding scaled-up superconducting quantum processors, npj Quantum Inf. **7**, 129 (2021).

[9] C. Berke, E. Varvelis, S. Trebst, A. Altland, and D. P. DiVincenzo, Transmon platform for quantum computing challenged by chaotic fluctuations, Nat. Commun. **13**, 2495 (2022).

[10] X. Xu, Manabputra, C. Vignes, M. H. Ansari, and J. Martinis, Lattice Hamiltonians and stray interactions within quantum processors, arXiv:2402.09145.

[11] D. A. Huse, R. Nandkishore, and V. Oganesyan, Phenomenology of fully many-body-localized systems, Phys. Rev. B **90**, 174202 (2014).

[12] M. Serbyn, Z. Papić, and D. A. Abanin, Local conservation laws and the structure of the many-body localized states, Phys. Rev. Lett. **111**, 127201 (2013).

[13] The reason for this bit flipping is the unfortunate convention in quantum information of having the ground state denoted by 1 and the first excited state by 0, which we do not adopt here.

[14] Chr. Møller and M. S. Plesset, Note on an approximation treatment for many-electron systems, Phys. Rev. **46**, 618 (1934).

[15] J. Koch, T. M. Yu, J. Gambetta, A. A. Houck, D. I. Schuster, J. Majer, A. Blais, M. H. Devoret, S. M. Girvin, and R. J. Schoelkopf, Charge-insensitive qubit design derived from the Cooper pair box, Phys. Rev. A **76**, 042319 (2007).

[16] J. Gambetta, *Quantum Information Processing, Lecture Notes of the 44th IFF Spring School* (Forschungszentrum Jülich, Jülich, 2013).

[17] T. Proctor, K. Rudinger, K. Young, E. Nielsen, and R. Blume-Kohout, Measuring the capabilities of quantum computers, Nat. Phys. **18**, 75 (2022).

[18] P. W. Anderson, Absence of diffusion in certain random lattices, Phys. Rev. **109**, 1492 (1958).

[19] F. Evers and A. D. Mirlin, Anderson transitions, Rev. Mod. Phys. **80**, 1355 (2008).

[20] S. Aubry and G. André, Analyticity breaking and Anderson localization in incommensurate lattices, Ann. Israel Phys. Soc. **3**, 18 (1980).

[21] Y. E. Kraus, Y. Lahini, Z. Ringel, M. Verbin, and O. Zilberberg, Topological states and adiabatic pumping in quasicrystals, Phys. Rev. Lett. **109**, 106402 (2012).

[22] G. Roati, C. D'Errico, L. Fallani, M. Fattori, C. Fort, M. Zaccanti, G. Modugno, M. Modugno, and M. Inguscio, Anderson localization of a non-interacting Bose-Einstein condensate, Nature (London) **453**, 895 (2008).

[23] A. Szabó and U. Schneider, Mixed spectra and partially extended states in a two-dimensional quasiperiodic model, Phys. Rev. B **101**, 014205 (2020).

[24] D. Johnstone, P. Öhberg, and C. W. Duncan, The mean-field Bose glass in quasicrystalline systems, J. Phys. A: Math. Theor. **54**, 395001 (2021).

[25] V. W. de Spinadel, The metallic means family and multifractal spectra, Nonlinear Anal. Theory Methods Appl. **36**, 721 (1999).

[26] I. V. Beloussov, Another formulation of the Wick's theorem. Farewell, pairing? Spec. Matrices **3**, 169 (2015).

[27] J. A. Pople, J. S. Binkley, and R. Seeger, Theoretical models incorporating electron correlation, Int. J. Quantum Chem. **10**, 1 (1976).